

## Observation of ordered structures of Sr on the Si(100) surface

W. C. Fan, N. J. Wu, and A. Ignatiev

*Department of Physics and the Space Vacuum Epitaxy Center, University of Houston, Houston, Texas 77204*

(Received 14 February 1990)

Several ordered structures due to Sr adsorption have been observed on the Si(100) surface by low-energy electron diffraction: (1) a  $(2 \times 3)$  phase, (2) a  $(1 \times 2)$  phase, (3) a compressed  $(1 \times 5)$  phase, and (4) a  $(1 \times 3)$  phase. The relationship between the ordered structures has been investigated as a function of Sr coverage and substrate annealing temperature. The data suggest that the Sr atoms form atomic chains on the surface, with spacing between the chains decreasing as Sr coverage increases.

### I. INTRODUCTION

The adsorption of metals on the Si(100)- $(1 \times 2)$  surface has been an area of significant effort in the study of metal-semiconductor interfaces due to a relatively simple atomic structure for the Si(100) surface. A variety of interface atomic structures of metal overlayers on the Si(100) surface have been already observed and studied with different surface techniques.<sup>1-6</sup> Among those ordered structures, one of particular interest is the atomic structure of alkali-metal overlayers<sup>2</sup> since it raises the possibility of one-dimensional (1D) metallization of atomic chains and the metallization of the dimerized surface of the Si(100) substrate.<sup>7,8</sup>

Furthermore, the interaction of certain metals such as Bi, Cu, and Sr with the surface of semiconductors such as silicon is of current importance due to major interest in integration of semiconductors and the new high-temperature superconductor (HTCS) materials such as the Bi-Sr-Cu-O compounds.<sup>9</sup> The low-energy electron diffraction (LEED) study reported here on the interaction of Sr atoms with the Si(100) surface is an attempt to illustrate the interaction of the elements of HTCS materials with Si. It will be shown that the Sr on the Si surface forms chain structures which may be related to those observed for alkali-metal-atom interaction with semiconductor surfaces.<sup>2</sup>

### II. EXPERIMENT

The experiment was carried out in an ultra high-vacuum (UHV) chamber equipped with a four-grid LEED optics and Auger-electron spectroscopy (AES) as described in a previous work.<sup>10</sup> The Si(100) sample was a piece of *p*-type wafer with resistivity  $\approx 80 \Omega \text{ cm}$  (B doped). The surface of the sample was cleaned by 1-keV  $\text{Ar}^+$ -ion bombardment followed by high-temperature annealing ( $\sim 1100^\circ\text{C}$ ), resulting in a clear  $(1 \times 2)$  LEED pattern and less than 0.5% surface contamination as determined by AES. The temperature of the sample was measured by an Alumel-Chromel thermocouple attached to the sample surface by a thin Ta-foil clamp. The Sr source was made from a piece of bulk Sr wound with tungsten

wire and heated electrically. The Sr deposition rate was calibrated by a quartz microbalance and controlled at about 0.1 ML/min [1 ML (monolayer) =  $6.8 \times 10^{14}$  atoms/cm<sup>2</sup>, equal to the atomic density of the Si(100) surface]. The vacuum in the chamber during the course of the experiment was better than  $2 \times 10^{-10}$  Torr.

### III. RESULTS AND DISCUSSIONS

The deposition of Sr on the Si(100)- $(1 \times 2)$  surface was first studied at room temperature with LEED. After Sr adsorption onto the room-temperature substrate, no long-range-ordered structures were observed. The intensity of the Si(100)- $(1 \times 2)$  structure of the substrate was, however, observed to decrease drastically with increasing Sr exposure, indicating adsorption of disordered Sr, i.e., no long-range order. However, short-range-ordered (SRO) structures of the Sr overlayer could not be excluded.

A number of long-range-ordered structures were, however, observed under high-temperature anneals after the adsorption of various amounts of Sr. As shown in Fig. 1(a), a  $(2 \times 3)$  LEED pattern was first observed after adsorption of about 0.3 ML Sr and an anneal for 1 min to about  $800^\circ\text{C}$ . This  $(2 \times 3)$  pattern was converted to a well-ordered  $(1 \times 2)$  pattern [Fig. 1(b)] after annealing to  $800^\circ\text{C}$  as the exposure reached about 0.5 ML. With increasing Sr exposure and  $800^\circ\text{C}$  annealing after the adsorption, the  $(1 \times 2)$  phase of the Sr overlayer remained a well-ordered  $(1 \times 2)$  structure, showing sharp LEED spots and low diffuse background, until an exposure of about 1 ML was reached.

At a Sr exposure of more than 1 ML, the  $(1 \times 2)$  phase of the Sr overlayer converted continuously to a  $(1 \times 5)$  phase [Fig. 1(d)] through an intermediate phase [Fig. 1(c)] which showed significant broadening in beam width. Further deposition and annealing of Sr onto the  $(1 \times 5)$  phase resulted in a  $(1 \times 3)$  phase [Fig. 1(e)]. At high Sr exposure ( $> 1.5$  ML), the LEED pattern was degraded with a decrease in coherent intensity and an increase in diffuse background. The LEED beams at noninteger positions became weak and streaky, indicating that disorder in the Sr overlayer was increasing.

The relationship between the observed Sr long-range-

ordered structures is described in Fig. 2 as a function of exposure and annealing temperature. The boundary between the ordered structures, as noted, is not clear-cut due to possible phase mixtures between the ordered phases. After Sr adsorption onto the clean Si(100)-(1×2) surface, an anneal at a temperature above that defined by the double-dashed lines in Fig. 2 can result in the respective ordered structure. However, better-ordered structures of the Sr overlayer are observed after annealing to a temperature which is near the desorption temperature indicated by a dashed curve in Fig. 2.

It is worthwhile to point out here that the annealing history of the Sr overlayer on the substrate may significantly affect the annealing temperature required to obtain an ordered structure of the Sr overlayer. For example, it is easier and requires much lower annealing temperature to obtain an ordered structure upon Sr adsorption onto the Si substrate if the substrate has already been exposed to Sr vapor and experienced a high-

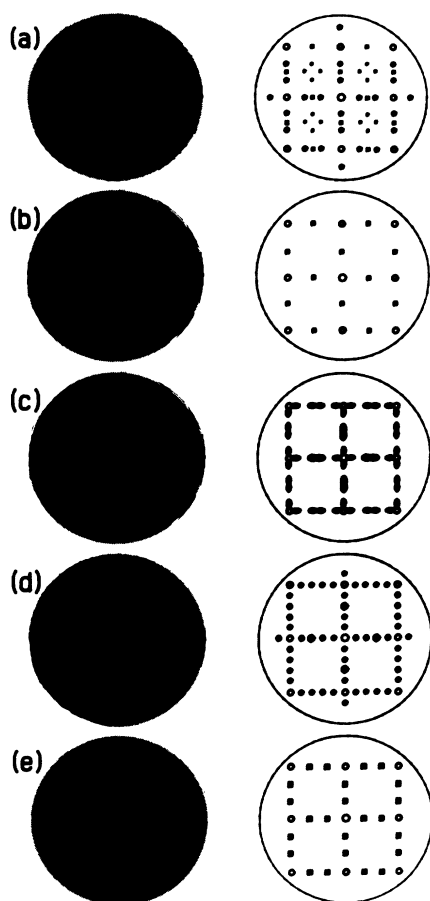


FIG. 1. LEED patterns and their schematic patterns for Sr overlayers on the Si(100) surface. (a) A (2×3) phase or a coexisting phase of a (1×2) and (1×3) phase at  $\Theta \approx 0.4$  ML and 50 eV; (b) a (1×2) phase at  $\Theta \approx 0.6$  ML and 50 eV; (c) an intermediate phase at  $\Theta \approx 1.1$  ML and 50 eV; (d) a (1×5) phase at  $\Theta \approx 1.2$  ML and 68 eV; (e) a (1×3) phase at  $\Theta \approx 1.3$  ML and 52 eV.

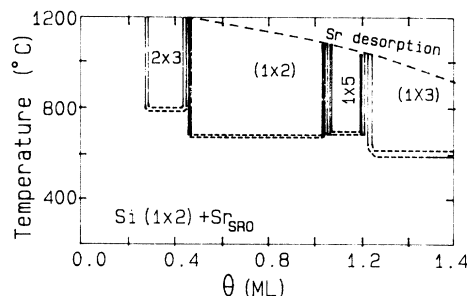


FIG. 2. Partial phase diagram for Sr on Si(100).  $Sr_{SRO}$  indicates possible short-range-ordered structures in the Sr overlayer.

temperature anneal. The anneal after initial Sr deposition ( $\approx 0.3$  ML) may weaken the dimer bonds of the Si surface and make the surface smoother, and thus enhance the Sr atomic mobility at high exposure.

According to the decreasing trend in the Sr deposition temperature with increasing coverage (Fig. 2), the bonding between Si and Sr is stronger at low coverage ( $< 0.5$  ML) and decreases continuously as coverage increases. The continuous variation of the bonding strength suggests that the bonding nature of Si and Sr could be partially ionic due to charge transfer to the Si substrate similar to alkali metals on Si surfaces.

In addition to the LEED-pattern observations discussed above, LEED-intensity measurements have been made in attempts to further understand each of the individual ordered phases. First, it is possible that the (2×3) phase is composed of both (1×2) and (1×3) phases, e.g., substrate and overlayer, respectively. As seen in the intensity profiles shown in Fig. 3 (left panel), the intensity

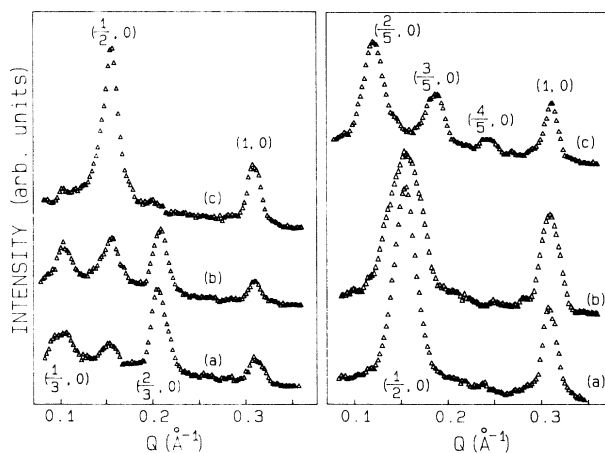


FIG. 3. Beam profiles along the [10] direction as a function of Sr coverage, for the transitions (left panel) from the (2×3) to the (1×2) phase [(a) to (c)] and (right panel) from the (1×2) to the (1×5) phase [(a) to (c)] as a function of increasing Sr coverage.

at the half-integer position increases with increase of coverage, while the  $(2 \times 3)$  phase converts to a  $(1 \times 2)$  phase. This indicates the coexistence of the  $(2 \times 3)$  and  $\theta \approx 0.5$  ML  $(1 \times 2)$  phase. For the low-coverage  $(2 \times 3)$  phase ( $\Theta \approx 0.35$  ML), the intensities at the half-integer positions are, however, relatively weaker than those at the one-third positions. This suggests that the weaker half-integer beams may be related to the  $(1 \times 2)$ -substrate reconstruction. The  $(2 \times 3)$  phase at lower coverage, therefore, could be a composite structure of  $(1 \times 3)$  Sr overlayer on the  $(1 \times 2)$  reconstructed substrate, in agreement with the coverage required for the  $(1 \times 3)$ -overlayer structure as determined by experiment.

The  $(1 \times 2)$  phase of the Sr overlayer, which was observed over a wide coverage range (Fig. 2), requires further LEED study to understand the intrinsic nature of the  $(1 \times 2)$  phase. The  $I$ - $V$  curves of the  $(1 \times 2)$  Sr phase were measured as a function of coverage. The  $I$ - $V$  curves show continuous changes in both peak shape and relative intensity. Even at low coverage ( $\Theta \approx 0.5$  ML), the  $I$ - $V$  curves are very different from those of the clean  $(1 \times 2)$  reconstructed silicon surface. The  $(1 \times 2)$  phase under Sr adsorption is, therefore, changing atomic structure as Sr coverage increases. It is highly probable that the  $(1 \times 2)$  Sr phase is composed of two types of  $(1 \times 2)$  domains with different local coverages of  $\Theta = 0.5$  ML and 1, respectively. The low-coverage  $(1 \times 2)$  phase is gradually replaced by a high-coverage  $(1 \times 2)$  phase with increasing Sr coverage.

The phase transition of the high-coverage  $(1 \times 2)$  phase to the  $(1 \times 5)$  phase is further revealed in the intensity profiles of Fig. 3 (right panel). The significant broadening in LEED beam width of both integer and noninteger beams is clearly shown in the profile for the phase intermediate between the ordered phases. This can be interpreted as a response to the mixing of the  $(1 \times 2)$  phase,  $(1 \times 5)$  phase, and possible incommensurate phase domains. The transition from the  $(1 \times 5)$  to the  $(1 \times 3)$  phase is also accompanied by a mixed phase, as a weak streak can still be seen near the  $(\frac{1}{3}, 0)$  beam in Fig. 1(e).

A unique picture of the various Sr-overlayer atomic structures can be constructed from the LEED observations based on Sr atomic chains. As shown in Fig. 4(a), the atomic structure for the  $(2 \times 3)$  phase is suggestive of  $(1 \times 3)$  Sr chains on a  $(1 \times 2)$  reconstructed substrate. The  $(1 \times 3)$  Sr chains could be perpendicular to the dimer chains of the Si(100)- $1 \times 2$  surface in which the dimer bonds might be weakened by the Sr adsorbate.

The structural model of the low-coverage  $(1 \times 2)$  Sr phase is constructed with simple  $(1 \times 2)$  Sr chains of  $\Theta = 0.5$  ML on a Si(100) surface [Fig. 4(b)]. The Sr structure of the high-coverage  $(1 \times 2)$  phase is proposed to be composed of dimer chains of Sr atoms ( $\Theta = 1$  ML), as shown in Fig. 4(c). The observed change of the  $(1 \times 2)$  Sr structure, as coverage increases, is probably a replacement of the single-chain  $(1 \times 2)$  structure with the dimer-chain  $(1 \times 2)$  structure. The spacing between the Sr chains can further decrease as coverage increases. The Sr atomic chains can be locked into the  $(1 \times 5)$  and  $(1 \times 3)$  modulations with respect to the Si(100)- $(1 \times 1)$  substrate at coverages of 1.2 and 1.3 ML, respectively, as shown in

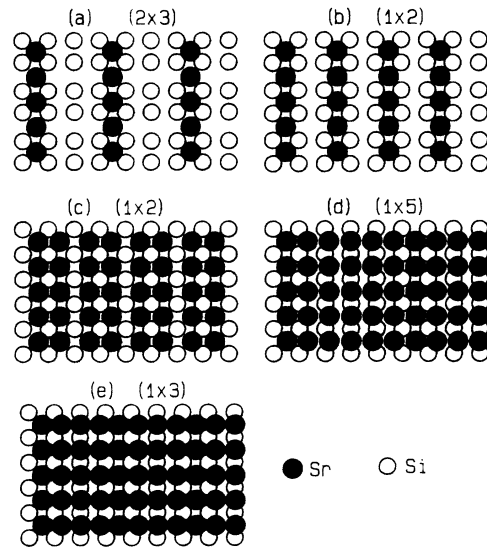


FIG. 4. Possible chain structures of Sr atoms in the overlayer on Si(100) surface. (a) A  $(1 \times 3)$  Sr structure with  $\Theta = \frac{1}{3}$  ML; (b) a  $(1 \times 2)$  structure with  $\Theta = 0.5$  ML; (c) a  $(1 \times 2)$  structure with  $\Theta = 1$  ML; (d) a  $(1 \times 5)$  structure with  $\Theta = 1.25$  ML; (e) a compressed  $(1 \times 3)$  structure with  $\Theta = \frac{4}{3}$  ML.

Figs. 4(b) and 4(e). However, the final proof of the proposed structural models requires LEED dynamical calculations.

Within the models of the Sr atomic structures in Fig. 4, the atomic spacing in the Sr overlayers is smaller than the atomic spacing in bulk Sr. In the compressed  $(1 \times 3)$  Sr overlayer, the atomic spacing between the Sr chains has reached a minimum of 2.9 Å, which is about 33% smaller than the bulk Sr atomic spacing (4.3 Å). This kind of reduction of the atomic spacing is due to charge transfer to the substrate and has been often observed in alkali-metal overlayers.<sup>11</sup>

Finally, the relationship of the Sr atomic structures (Fig. 2) can probably shed light on the study of the HTSC thin films of Bi-Sr-Cu-O compound. The initial Sr deposition and substrate temperature may be vital to the growth of the single-crystal films of the HTSC material on the Si(100) surface. Since the ordered Sr structures can only result from a Sr overlayer of low coverage ( $< 1.5$  ML) at high temperature, excessive amounts of Sr deposition could be destructive to the HTSC crystal-film growth on the Si substrate.

#### IV. CONCLUSIONS

Long-range ordered structures defined as  $(2 \times 3)$ ,  $(1 \times 2)$ ,  $(1 \times 5)$ , and  $(1 \times 3)$  phases have been observed with LEED after exposure and annealing of the Si(100)

surface to Sr. The partial phase diagram has been developed for the system and indicates long-range Sr overlayer ordering to coverages up to about 1.4 ML. From the LEED observation, the ordered structures are proposed to be based on Sr chain structures in the adsorbed and annealed overlayers.

#### ACKNOWLEDGMENTS

This work is supported in part by the R. A. Welch Foundation (Houston, TX) the U.S. National Aeronautics and Space Administration, and the Texas Center for Superconductivity at the University of Houston.

---

<sup>1</sup>Some earlier work can be found in Refs. 2–6.

<sup>2</sup>T. Abukawa and S. Kono, *Surf. Sci.* **214**, 141 (1989).

<sup>3</sup>D. H. Rich, T. Miller, A. Samasvar, H. F. Lin, and T.-C. Chiang, *Phys. Rev. B* **37**, 10221 (1988).

<sup>4</sup>T. Kendelewicz, P. Soukiassian, R. S. List, J. C. Woicik, P. Pianetta, I. Lindau, and W. E. Spicer, *Phys. Rev. B* **37**, 7115 (1988).

<sup>5</sup>R. D. Bringans and M. A. Olmstead, *Phys. Rev. B* **39**, 12985 (1989).

<sup>6</sup>J. Zegenhagen, J. R. Patel, B. M. Kincaid, J. A. Golovchenko, J. B. Mock, P. E. Freeland, R. J. Malik, and K.-G. Huang,

*Appl. Phys. Lett.* **53**, 252 (1988).

<sup>7</sup>Y. Ling, A. J. Freeman, and B. Delley, *Phys. Rev. B* **39**, 10144 (1989).

<sup>8</sup>S. Ciraci and I. Batra, *Phys. Rev. B* **37**, 2955 (1988).

<sup>9</sup>H. Maeda, Y. Tanaka, M. Fukutoma, and T. Asano, *Jpn. J. Appl. Phys. Lett.* **27**, L209 (1988).

<sup>10</sup>W. C. Fan and A. Ignatiev, *Phys. Rev. B* **40**, 5359 (1989).

<sup>11</sup>A. Ignatiev and W. C. Fan, *J. Vac. Sci. Technol. A* **4**, 1415 (1986); W. C. Fan and A. Ignatiev, *Phys. Rev. B* **37**, 5274 (1988).

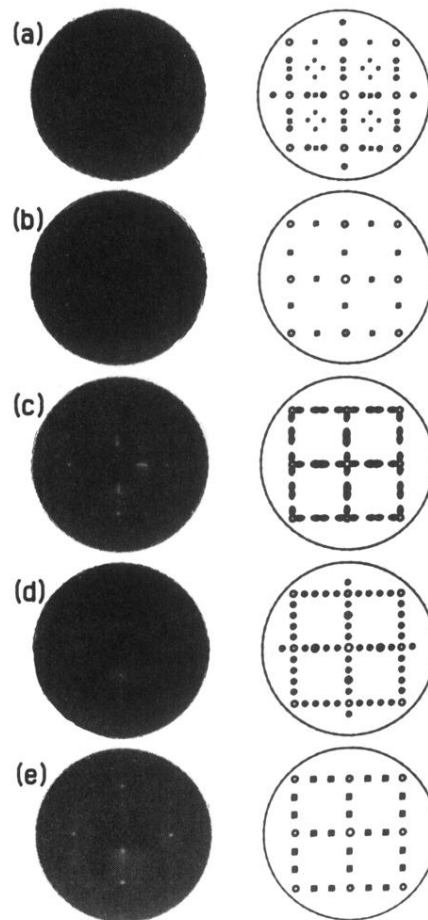


FIG. 1. LEED patterns and their schematic patterns for Sr overlayers on the Si(100) surface. (a) A  $2 \times 3$  phase or a coexisting phase of a  $1 \times 2$  and  $1 \times 3$  phase at  $\Theta \approx 0.4$  ML and 50 eV; (b) a  $1 \times 2$  phase at  $\Theta \approx 0.6$  ML and 50 eV; (c) an intermediate phase at  $\Theta \approx 1.1$  ML and 50 eV; (d) a  $1 \times 5$  phase at  $\Theta \approx 1.2$  ML and 68 eV; (e) a  $1 \times 3$  phase at  $\Theta \approx 1.3$  ML and 52 eV.